THE JOURNAL OF PHYSICAL CHEMISTRY C

Article

pubs.acs.org/JPCC

Precision of Electric-Field Gradient Predictions by Density Functional Theory and Implications for the Nuclear Quadrupole Moment and Its Error Bar of the ^{111}Cd 245 keV 5/2$^+$ Level

Leonardo Errico,[†,‡] Kurt Lejaeghere,[§] Jorge Runco,[†] S. N. Mishra,[⊥] Mario Rentería,[†] and Stefaan Cottenier*[,§,∥]

[†]Departamento de Física and Instituto de Física La Plata (IFLP, CCT-La Plata, CONICET-UNLP), Facultad de Ciencias Exactas, Universidad Nacional de La Plata, Casilla de Correo 67, 1900 La Plata, Argentina

[‡]Universidad Nacional del Noroeste de la pcia. de Buenos Aires (UNNOBA), Monteagudo 2772, Pergamino, (CP 2700) Buenos Aires, Argentina

[§]Center for Molecular Modeling, and [∥]Department for Materials Science and Engineering, Ghent University, Tech Lane Ghent Science Park − Campus A, building 903, BE-9052 Zwijnaarde, Belgium

[⊥]Tata Institute of Fundamental Research, Homi Bhabha road, Mumbai-400005, India

ABSTRACT: We present ab initio calculated electric-field gradient tensors at Cd sites in a set of simple yet diverse noncubic metals. By combining these predictions with carefully selected published experimental data, the nuclear quadrupole moment of the 245 keV 5/2$^+$ level of ^{111}Cd is determined to be 0.76(2) b. Knowing this quadrupole moment is important for time-differential perturbed angular correlation spectroscopy: decades of experimentally obtained nuclear quadrupole coupling constants for solids can now be more reliably converted into electronic structure information. For nuclear physics systematics, this is a rare opportunity to have reliable quadrupole moment information for a short-lived level that is not accessible to regular experimental methods. Much effort is spent on the determination of a meaningful error bar, which is an aspect that gained only recently more attention in the context of density functional theory predictions. This required assessing the numerical uncertainty in density functional theory predictions for electric-field gradient tensors in solids. In contrast to quantum chemistry methods, these density functional theory predictions cannot detect systematic errors. By comparing our quadrupole moment value with an independent value obtained from quantum chemistry calculations and experiment, we show that systematic errors are small for the systems studied here. Yet, there are indications that density functional theory underestimates by a few percent the electric-field gradient, and therefore overestimates the quadrupole moment by the same amount. We point out which future work needs to be done to characterize the possible deviations inherent to density functional theory.

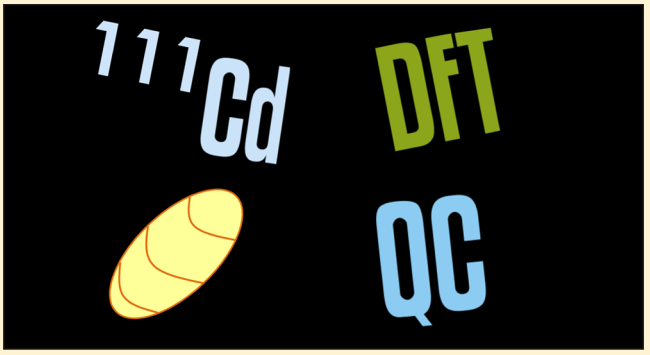

INTRODUCTION

The existence of a particularly convenient isotope is often the enabler of an experimental method that probes molecular or solid-state properties by the interaction of local electromagnetic fields with nuclear moments. Nuclear magnetic resonance[1] (NMR), for instance, would be much less useful if the magnetic moment of the proton (^{1}H) were smaller than it actually is. Mössbauer spectrosocopy[2] would be a marginal method if it were not for the ^{57}Fe nucleus with its exceptionally favorable compromise between many requirements. Similarly, time-differential perturbed $\gamma-\gamma$ angular correlation spectroscopy[3,4] (TDPAC), which is of interest in this Article, would be less useful without the 245 keV 5/2$^+$ level of ^{111}Cd as its work horse. Like the other above-mentioned experimental methods, the quantities that TDPAC measures depend both on a property of a nucleus and a property of the electron cloud in the studied solid or molecule. In particular, the electric quadrupole interaction frequency ν_Q, also known as the "quadrupole coupling constant", depends on both the spectroscopic nuclear quadrupole moment Q of the relevant nuclear level and the gradient of the local electric field at the site of the nucleus, V_{zz}:

$$\nu_Q = \frac{eQV_{zz}}{h} \tag{1}$$

where e is the electron charge, and h is Planck's constant. For many purposes, knowledge of the experimental quadrupole interaction frequency ν_Q is sufficient, and there is no need to

Received: June 17, 2016
Revised: September 6, 2016
Published: September 6, 2016

DOI: 10.1021/acs.jpcc.6b06127
J. Phys. Chem. C 2016, 120, 23111−23120

disentangle it in nuclear and solid-state information. This happens, for instance, when one merely wants to label different lattice sites of an impurity atom in a solid,[5−10] or to identify phase transitions.[11−13] However, when one wants to use the method to experimentally determine the electric-field gradient (EFG) tensor in a solid, it is mandatory to have precise knowledge about the nuclear quadrupole moment Q. The latter is usually the bottleneck: the error bar on experimental quadrupole interaction frequencies can be better than 0.1%, whereas nuclear quadrupole moments are typically known up to one or two digits only, often with an unspecified error bar.[14−17]

This rather imprecise knowledge of nuclear quadrupole moments has spurred several initiatives during the past two decades to apply ab initio electronic structure methods for the benefit of nuclear moment determination. It is nowadays routinely possible to compute the electric-field gradient tensor in solids from first principles. The absolute accuracy of this computed/predicted field gradient does by far not reach the same level as for experimental quadrupole interaction frequencies yet, but is definitely better than the 1−2 digit precision of experimental nuclear quadrupole moments. Equation 1 shows that Q then can be obtained from the slope of a linear fit through a data set of calculated values of V_{zz} versus experimental values for ν_Q (see also Figure 1), yielding a much improved precision. The uncertainty on the resulting Q is mainly determined by the accuracy of the ab initio calculations. Many quadrupole moments have been determined in this way.[18−26]

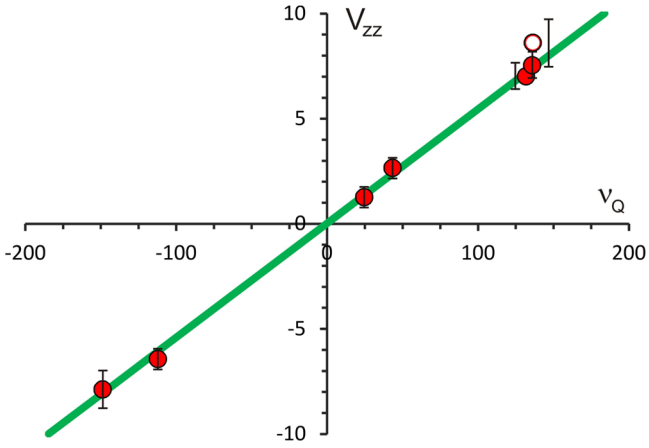

Figure 1. Ab initio calculated principal component V_{zz} of the electric-field gradient (EFG) tensor (10^{21} V/m^2) versus experimental quadrupole interaction frequency ν_Q (MHz). These data are listed in Table 1 as well. The error bars on ν_Q vary between 0.1 and 2 MHz, and are not visible on this scale. The error bars on V_{zz} are horizontally shifted for some data points, for clarity. The "○" indicate data points that were determined to be outliers by the procedure described in the section on Outlier Assessment. The fitted linear correlation takes into account the inliers (red ●) only, and corresponds to the fit parameters listed in Table 2, second column.

Whereas the combination of quadrupole interaction frequency measurements and ab initio calculations does provide fair values for nuclear quadrupole moments, it remains unclear how large the uncertainty of the obtained quadrupole moments is when this procedure is used. A rule of thumb of 10−20% is sometimes quoted,[18,19,21,24] yet the origin of this number is unclear and certainly not based on rigorous testing. The goal of this Article is to examine meticulously the various sources of errors for one particular case where a high precision is essential: the quadrupole moment of the 245 keV level in ^{111}Cd (I^π = 5/2$^+$), because this is an important isotope, dominantly used in TDPAC experiments.

Attempts to determine this quadrupole moment date back to 1962, and have been reviewed by van der Werf et al.[27] and by Haas and Correia.[25] These and some additional data points have been summarized in Figure 2. The data and their error bars cover the range from 0.3 to 1.9 b, with most data clustering around 0.8 b. According to the assessement of ref 25, the five data points labeled by filled circles are sound measurements (in contrast to the open circles, which are experimental estimates). Among those, the highest value of 1.5 b is an obvious outlier. The average of the four remaining experimental values is 0.80 b, and the error bar on the average is 0.07 b (determined as $\sqrt{\sum \varepsilon_i^2}/N$). This experimental range is indicated by the shaded bar in Figure 2. Rather than using this combined value of 0.80(7) b, it has become common practice in the literature to quote the 0.83(13) b by Herzog et al.[28] as the accepted value for Q. A few authors defend a slightly lower value around 0.78 b.[29,30] The recent tabulation by N. J. Stone[17] of recommended values for quadrupole moments favors 0.74(7) b (the one from ref 31). In the original paper, the value of Herzog et al. is claimed to have been obtained in a "model-independent way", by measuring the quadrupole interaction frequencies for two different ^{111}Cd levels (5/2$^+$ and 11/2$^-$) in the same host material (hcp-Zn). It is an immediate consequence of eq 1 that the quadrupole moment of the 5/2$^+$ level can be determined if the quadrupole moment of the 11/2$^-$ level is known:

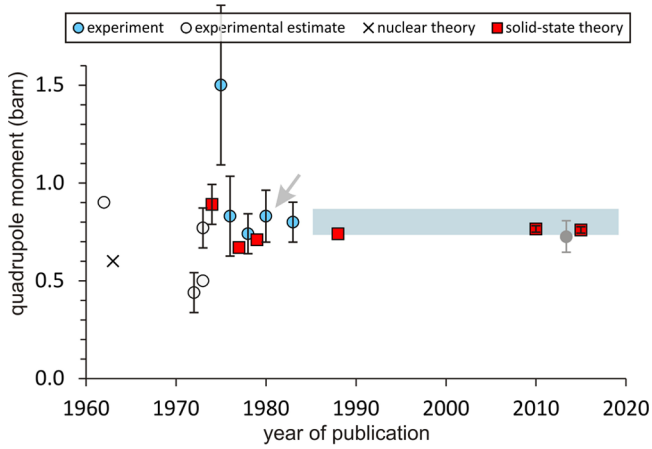

Figure 2. Overview of experimental (circles) and theoretical (crosses and squares) determinations of the quadrupole moment Q of ^{111}Cd (5/2$^+$). These data have been listed and/or reviewed in refs 14, 25, and 27, and the original data are from refs 25, 28, 31, 33−44. The open circles indicate experimental values that were merely estimates, following the assessment of ref 25. The 1975 experimental value of 1.5 b is an obvious outlier. The shaded horizontal bar shows the range of 0.80(7) b that is determined by the other four reliable experimental data points. The commonly quoted value of 0.83(13) b is indicated by an arrow. The gray circle at the right is a reanalysis of the latter value based on a 2013 result for a reference quadrupole moment[45] (see text). The most recent solid-state theory data point is from this work, including an in-depth error analysis (the error bar is drawn inside the red square).

DOI: 10.1021/acs.jpcc.6b06127
J. Phys. Chem. C 2016, 120, 23111−23120

Table 1. Seven Crystals Where the Quadrupole Interaction Frequency at a ^{111}Cd Nucleus Has Been Measured by TDPAC[a]

host lattice		lattice parameters	T_{abc}	ν_Q	$T_{\nu Q}$	supercell	$R_{mt}K_{max}$	k-points	V_{zz}
Ga	(64)	a = 4.5151, b = 4.4881, c = 7.6318[52]	2.35	−148.6(1)[53]	4.2	3 × 3 × 3	8	1000	−7.89(90)
Hg	(166)	a = 3.4573, c = 6.6636 (hex)[54]	5	−112(2)[37]	77	4 × 4 × 2	8	1000	−6.45(50)
bct-In	(139)	a = 3.221, c = 4.933[55]	4.2	24.82(20)[56]	1.2	4 × 4 × 3	8	1000	1.25(50)
β-Sn	(141)	a = 5.81187, c = 3.15743[57]	4.2	43.56(30)[56]	1.2	2 × 2 × 3	8	3000	2.65(50)
Sb	(166)	a = 4.3007, c = 11.222 (hex)[58]	4.2	132(3)[56,59]	77	3 × 3 × 2	8	2000	7.0(6)
Cd	(194)	a = 2.96313, c = 5.51890[25]	0	136.02(40)[56]	0.130	1 × 1 × 1	9	40 000	7.53(60)
Zn	(194)	a = 2.6588, c = 4.8515[60]	0	136.5(1.0)[61]	4.2	5 × 5 × 4	8	250	8.6(1.1)

[a]The columns list subsequently the lattice (space group ITA number is mentioned in parenthesis), the low-temperature experimental lattice parameters (Å), the temperature at which these lattice parameters were measured (K) ("0 K" refers to a reliable extrapolation to zero kelvin), the experimental quadrupole interaction frequency ν_Q (MHz, eq 1), the temperature at which the latter was measured (K), the supercell that has been used in the most accurate calculation, basis set size ($R_{mt}K_{max}$ or RKM) and k-mesh for Brillouin zone sampling that have been used in the most precize calculation, and the resulting ab initio calculated principal component V_{zz} of the electric-field gradient tensor (10^{21} V/m^2, LDA functional). The asymmetry parameter η is zero by symmetry in all cases, except for Ga (exp, 0.197;[53] LDA, 0.17).

$$Q(5/2^+) = Q(11/2^-)\frac{\nu_Q(5/2^+)}{\nu_Q(11/2^-)} \quad (2)$$

The reliability of the obtained value is limited by the reliability of the known $11/2^-$ quadrupole moment, which is in this case a result from optical double resonance spectroscopy in combination with an estimate for the $\langle r^{-3}\rangle$ of the $p_{3/2}$-electron in Cd (−0.85(9) b from ref 32). Calling this a "model-independent result" is therefore not really justified. The most recent theoretical data point (apart from the present work) in Figure 2 is by Haas and Correia,[25] based on ab initio calculations for the electric-field gradient in hcp-Cd. Their value of 0.765(15) b is consistent with the experimental values, yet is claimed to be an order of magnitude more precise. We will discuss this claim in the Discussion and Conclusions, and compare it with our approach.

The subject of this Article fits in a recent trend in the field of DFT applications to determine error bars on DFT predictions of various observable quantities[46−51] in a more rigorous way. As will be elaborated upon in the section on Linear Correlation, a distinguishing feature of the present work is that the property of interest (Q) can be distorted by a systematic bias in the DFT predictions that is undetectable. This undetectability will limit the amount of knowledge that can be collected about the error bar on DFT-based quadrupole moments.

DATA SET

As we aim for the highest accuracy and precision, a limited set of simple yet diverse solids was taken for which accurate experimental information on structural parameters and quadrupole interaction frequencies at low temperature are available, and for which precise ab initio calculations could be performed. The final data are collected in Table 1 and Figure 1. The important issue of error bars on these data will be discussed in the section on the Error Budget.

Experimental Section. For all seven crystals shown in Table 1, the experimental quadrupole interaction frequency ν_Q as determined by the TDPAC method at low temperature can be found in the literature. Low-temperature values are essential because these will have to be compared to ab initio calculations at 0 K. Crystals for which only room-temperature values for ν_Q are available are not of any use here: the temperature dependence of the quadrupole interaction in the range 0−300 K is considerable and cannot be universally parametrized,[62−68] such that room-temperature values for ν_Q cannot be reliably converted into 0 K values. On the other hand, papers that do report low-temperature ν_Q values do not usually report (accurate) low-temperature lattice parameter data for the same samples. As the latter is essential input information for the ab initio calculations, these low-temperature lattice parameters have been collected from dedicated crystallographic literature and are reported in Table 1 as well.

Computational. DFT can predict ground-state (=0 K) lattice parameters of solids with considerable accuracy. In a general error bar assessment for structural properties of solids, Lejaeghere et al.[47] showed that DFT calculations with a common GGA exchange-correlation functional systematically overestimate the ground-state volume per atom by 3.8%, with a remaining scatter (or error bar) of 1.1 Å^3/atom. It would therefore be perfectly possible to predict the ground-state lattice parameters of these seven crystals ab initio, and then compute the electric-field gradient tensor for these ab initio predicted structures. That would be a truly ab initio prediction of the electric-field gradient tensor. When it comes to extracting the quadrupole moment Q, however, what one needs is not in the first place a rigorous ab initio prediction of the electric-field gradient, but rather a prediction that comes as close as possible to the true experimental value. Using predicted lattice parameters that do deviate, albeit only slightly, from experiment would mean that a deviation of the predicted EFG is already built-in into the procedure. This holds a fortiori for the c/a ratio, which directly influences the EFG.[25] It is therefore more appropriate for our present purpose to start from the experimental low-temperature lattice parameters, and compute the EFG for that lattice.

The DFT code used for the EFG calculations was WIEN2k,[69] a code with a long tradition in EFG predictions.[18,44,70−76] It solves the scalar-relativistic Kohn−Sham equations using an Augmented Plane Waves + local orbitals (APW+lo) basis set.[77−79] In this method, the wave functions are expanded into spherical harmonics inside nonoverlapping atomic spheres of radius R_{MT} and in plane waves in the remaining space of the unit cell (=the interstitial region).

The plane-wave expansion of the wave function in the interstitial region was truncated at very large wave numbers K_{max} = RKM/R_{MT}^{min} (values of RKM are listed in Table 1). A very dense mesh of k-points (listed in Table 1) was used for Brillouin zone integration. Several exchange-correlation functionals were considered (see the section on Error Budget). To mimic the situation of isolated Cd impurity atoms, the actual unit cells in our calculations were supercells: $m \times n \times k$ multiplications of a primitive unit cell, in which one of the host

DOI: 10.1021/acs.jpcc.6b06127
J. Phys. Chem. C 2016, 120, 23111−23120

lattice atoms is replaced by the Cd impurity. All atoms in the supercell were allowed to completely relax to new equilibrium positions (keeping the lattice parameters fixed), to accommodate for the presence of the impurity atoms.

ANALYSIS

Outlier Assessment. To obtain Q, we need to determine the slope of a linear fit through the calculated V_{zz} data versus the experimental ν_Q data (Figure 1, and the ν_Q and V_{zz} columns in Table 1). Two extreme situations might occur (see Figure 3).

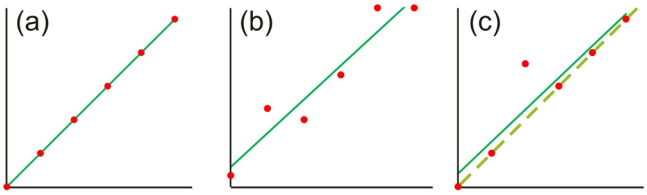

Figure 3. Depending on the properties of the data points (red circles), different approaches are needed to extract the maximum amount of information from the data. A linear fit (full line) is appropriate for either ideal data points (a), or for data sets where all data points show a similar amount of scatter (b). In case a few data points are clear outliers (c), a linear fit through all data points distorts the available information. If the outlier can be removed first, a linear fit through the remaining data points reveals the underlying information better (dashed line).

(a) If all data points neatly fall on a straight line, then the slope can be determined with high reliability. (b) If all data points are randomly scattered along an (unknown) ideal line, then the slope of the fitted line has an inherent uncertainty, yet that uncertainty is robust against removing, adding, or changing one data point. Both situations would lead to acceptable conclusions. Additional effort is needed, however, in this situation: (c) Most data points fall perfectly on a straight line, while one point (or a few) clearly is an outlier. A straightforward linear fit through such a data set would result in a distorted estimate for the slope and an error bar for the slope that is mostly determined by the deviating point. The value for the slope would therefore be less precise than the data actually justify. A much more precise value could be obtained if the outlier were removed first. This leads to the question: how to recognize outliers in an objective and statistically justified way? Obviously one wants to avoid biasing the fit by subjectively removing data points one does not like.

An objective procedure to detect outliers has been described in ref 80, and a similar approach has been applied to the present data set. In particular, a linear weighted least-squares fit with zero intercept was performed on the data of Figure 1 or Table 1, temporarily neglecting the small error bar on the experimental ν_Q. Data points with a studentized residual corresponding to a two-sided p-value of 0.05 or less were flagged one by one and removed until no such outliers could be detected anymore.[81] Note that a more advanced regression[82,83] is employed to estimate the final regression parameters in the section on Linear Correlation, which does take the small errors on ν_Q into account. Given the latter errors being small, however, a simpler weighted least-squares fit suffices for the purpose of outlier identification, while still allowing a statistical justification. The results of this outlier analysis are reported in Table 2. When all seven data points are taken into account (left column of Table 2), the two-sided p-value for Zn is below the threshold of 0.05, flagging it as an outlier. Repeating the analysis for the six data points without Zn (right column) shows no value below the threshold any longer. This objective removal of the Zn data point resembles scenario (c) in Figure 3, and is consistent with what a subjective analysis of Figure 1 would suggest: the Zn data point does not fit in the linear trend. What are the implications? The linear correlation from eq 1 is a law of nature: deviations from linearity can appear only by a hexadecapole contribution[84] or a quadrupole shift,[85−87] both being extremely small effects that cannot be noticed at the present level of experimental and theoretical accuracy. Therefore, either the experimental ν_Q or the calculated V_{zz} value for Zn must be incorrect. We did indeed observe that the calculated V_{zz} value for hcp-Zn is extremely sensitive to details: in contrast to all other examined crystals, V_{zz} kept changing with supercell size, even when very high numerical precision was requested for every individual calculation. We therefore had to assign a much larger error bar to this computed V_{zz}, even though the 5 × 5 × 4 supercell with 200 atoms was by far the largest one considered here (see also the section on Error Budget).

Table 2. Two-Sided p-Values for the Outlier Analysis, Applied to All Seven Data Points (Left Column) As Well As to the Data Points without Zn (Right Column)[a]

	all data	no Zn
Ga	0.214	0.306
Hg	0.910	0.158
In	0.828	0.751
β-Sn	0.816	0.324
Sb	0.407	0.496
Cd	0.741	0.560
Zn	**0.021**	
R^2	0.9986	0.9992
slope	0.056(2)	0.054(1)
intercept	0.2(2)	0.01(3)
Q (b)	0.74	**0.76**
error (b)	±0.03	**±0.02**

[a]The lower half of the table gives for the ($x = \nu_Q$, $y = V_{zz}$)-graph the correlation coefficient of the linear fit, the fitted slope and intercept with their error bars (determined by the method of refs 82 and 83), and the quadrupole moment deduced from the slope with its error bar.

Error Budget. The data points in Figure 1 and in Table 1 have error bars. Whereas this is normal for experimental values, it is less obvious for DFT predictions. We therefore discuss in the following how these error bars have been determined.

The error bars on the experimental quadrupole interaction frequencies ν_Q have been copied from the original experimental papers. In most cases, these papers do no mention a formal justification of the error bars. It is common practice in TDPAC experiments, however, to report the regression error bar on the frequency. This is obtained in the same way as for linear regression, but now for the so-called time-dependent correlation function[3,4] $R(t)$ that is fitted through an experimental time series of a few hundred points. Systematic experimental errors that are due to temperature calibration, frequency calibration, detector properties, etc., are hardly ever incorporated in this error bar. Although we will use the experimental error bars as reported, they are therefore definitely underestimations of the true error.

Error bars on DFT predictions are not common at all.[47,80] How do they arise? DFT as a formal method is exact, and

DOI: 10.1021/acs.jpcc.6b06127
J. Phys. Chem. C 2016, 120, 23111−23120

should provide absolutely accurate predictions. In practice, however, a choice has to be made for the so-called exchange-correlation functional. This leads to deviations between reality and DFT predictions (called "intrinsic errors" in ref 47). We have calculated the EFG for the considered seven crystals with three different choices of the exchange-correlation (LDA,[88] Wu−Cohen[89] (WC), and PBE-sol[90]). This led to a spread in EFG values of $\pm 0.10 \times 10^{21}$ V/m^2. It is important to realize that this bears no guarantee at all that the EFG predicted using the unknown exact exchange-correlation functional would be within this margin. This is a limitation in confidence that is inherent to DFT. Only a comparison with very accurate experimental values for V_{zz}, or with high-level quantum chemistry methods (provided they can be applied to metallic solids), would reveal the presence of this intrinsic error. This would require knowledge of the quadrupole moment, however, and this is exactly what we are trying to determine here. The true value of the intrinsic error can therefore not be known for this case.

Once a choice is made for the exchange-correlation functional in DFT, the Kohn−Sham equations are fully determined. A DFT code solves those numerically, and in principle this leads to solutions/predictions that are numerically exact. Settings of this numerical procedure will introduce some noise, though (called "numerical errors" in ref 47). The settings that are most important for keeping the numerical errors small are the basis set size and the density of the mesh used for Brillouin zone sampling. By examining the effect on the EFG of various basis set sizes and sampling meshes for these seven crystals, we find a spread of $\pm 0.05 \times 10^{21}$ V/m^2. Another feature that affects the predicted EFG is the distance between two Cd impurities, that is, the supercell size. This distance should be "infinite" (=100 Å or more), but is limited in practice to 10−20 Å. By systematically scanning several supercell sizes for these seven crystals, we estimate the supercell size effect on the EFG to be $\pm 0.10 \times 10^{21}$ V/m^2. An exception is hcp-Zn, where even a very large $5 \times 5 \times 4$ supercell (200 atoms) was not sufficient at all to converge the EFG to this level. We therefore adopt a supercell size contribution of $\pm 0.50 \times 10^{21}$ V/m^2 for the error on the EFG for Cd in hcp-Zn. Another source of uncertainty on the EFG is the choice of the lattice parameters, and, in particular, the c/a ratio. These should correspond to the low-temperature values valid for the sample on which the ν_Q measurement was done. For each of the seven crystals, we have calculated the EFG for several c/a ratios in an interval of ±0.75% around the experimentally observed c/a ratio that can be obtained from Table 1. This gave a linear variation of the EFG, with a slope that is different for each crystal. We then took a conservative estimate of 0.5% for the uncertainty in c/a ratio, and assigned a crystal-dependent uncertainty of the EFG to every crystal, ranging from $\pm 0.08 \times 10^{21}$ V/m^2 (In) to $\pm 0.35 \times 10^{21}$ V/m^2 (Zn). A final source of error is due to neglecting zero-point corrections to the calculated V_{zz}. For the case of hcp-Cd, this contribution was reported[68] to be 0.1×10^{21} V/m^2, by ab initio molecular dynamics. We added this value as a constant to all error bars. Although there have been several studies that showed how spin−orbit coupling can affect the electric-field gradient,[91−95] tests for the two host lattices with heavy elements (hcp-Cd and hcp-Hg) showed a negligible influence on V_{zz} for a Cd impurity (0.004 and 0.03×10^{21} V/m^2, respectively). Therefore, no error bar contribution due to neglecting spin−orbit coupling was considered.

The total error bar on the predicted EFG that is mentioned in Table 1 was then taken as the sum of the five contributions discussed in the previous paragraphs (0.10 + 0.05 + 0.10 + the crystal-dependent c/a-induced uncertainty +0.10). In this way, we obtain a conservative upper bound for the error, as it is unclear how the different error contributions are correlated. The conclusion is that the uncertainty on the predicted EFG is in the range $(0.4-0.7) \times 10^{21}$ V/m^2 (with Zn as a pathological exception: 1.1×10^{21} V/m^2). When expressed as a relative error bar, this corresponds to 5−10% for "large" EFGs ($>5 \times 10^{21}$ V/m^2) and 20−30% for "small" EFGs ($<3 \times 10^{21}$ V/m^2).

These uncertainties for ab initio calculated EFGs can be straightforwardly compared to recent post-Hartree−Fock calculations of the EFG in the $^3P_2$ and $^2P_{3/2}$ states of the free Cd atom.[45,96] Such calculations do not suffer from the choice of an exchange-correlation functional, nor do they require progressively larger supercells. The accuracy is determined by the number and type of "substitutions" of the reference configuration state function that are taken into account. The more substitutions are considered, the better the exact value of the EFG is approximated. Constraints on computing time determine how closely one can approach exactness. In ref 45, the EFG at the Cd nucleus in the $^2P_{3/2}$ state of the Cd atom was calculated to be $V_{zz} = (27.5 \pm 1.1) \times 10^{21}$ V/m^2. In ref 96, a value of $V_{zz} = (20.7 \pm 1.2) \times 10^{21}$ V/m^2 was found for the $^3P_2$ state. The absolute uncertainties of these numbers are twice as large as the uncertainties found in the present work, yet this is not surprising as the magnitude of the V_{zz} is substantially larger. The relative errors are 4% and 6%, respectively. This is in agreement with the relative error found in the present work for (very) large V_{zz}. We can therefore state that the error bar (precision) of these two very different theoretical methods is comparable. This does not imply that density functional and quantum chemistry methods must necessarily yield identical values for the EFG when applied to the same system. Comparisons between these classes of methods were made by Hemmingsen et al., who examined the EFG at the Cd nucleus in the $CdCl_2$ molecule. They found[29,30] two highly accurate quantum chemistry methods (MP2 and CCSD(T)) to provide nearly the same large value of about -30.4×10^{21} V/m^2. Density functional theory, on the other hand, gave a V_{zz} that is 20% smaller for the B3LYP functional (EFG calculated in ref 30). A comparable reduction was observed with a GGA functional (similar to the WC and PBEsol functionals used in the present work, EFG calculated in ref 97). Somewhat smaller deviations in the same direction were observed in Hg-containing molecules, where electric-field gradients obtained by nonrelativistic DFT were consistently a few percent smaller than the corresponding CCSD(T) values.[98] The crystals studied in the present work are more isotropic (i.e., they have a smaller V_{zz}) than the $CdCl_2$ molecule. Therefore, it is relevant to inspect the difference between quantum chemistry methods and DFT in more isotropic environments as well. In ref 30, V_{zz} on Cd was calculated for the CGI and TTC complexes. MP2 provides a V_{zz} of -5.6×10^{21} and 10.6×10^{21} V/m^2, respectively. The V_{zz} by DFT with the B3LYP functional is 1.0×10^{21} and 1.4×10^{21} V/m^2 smaller in absolute value. The relative difference is comparable to what is given hereabove for less isotropic systems, yet the absolute difference is smaller. If these observations for molecules would hold for crystals as well, and if one accepts that the V_{zz} determined by quantum chemistry methods is indeed closer to the exact value than the DFT value, then the quadrupole moment as determined by

DOI: 10.1021/acs.jpcc.6b06127
J. Phys. Chem. C 2016, 120, 23111−23120

DFT in the present work would be overestimated by up to 10−20%. A way to test this will be described in the Discussion and Conclusions.

Linear Correlation. Many basic as well as advanced data analysis packages provide routines to perform linear regression fits. In many of these, however, either no error bars on the data points are taken into account, or only error bars on the *Y*-variable, and often it is not explicitly documented what exactly has been implemented. In the present case, one wants to take into account error bars on the *X*-axis as well as on the *Y*-axis (Table 1 and Figure 1), and we want to be sure what the final error bar on the quadrupole moment really means. We have therefore implemented the formalism described by Borcherds, Ngwengwe, and Sheth[82,83] to perform linear regression on data with *X* and *Y* error bars, including a well-defined variance on the fitted parameters. The resulting values for the slope and intercept of the linear regression fit are given in Table 2, together with their error bars. According to eq 1, the intercept should be zero; this is consistent with Table 2, where the interval for the intercept does cover zero. Equation 1 is eventually used to convert the fitted slope into a quadrupole moment, including a value for its error bar. This error bar decreases upon the removal of the deviating data point for Zn. The final value of $Q = 0.76(2)$ b is the central result of this work. The significance of this result in relation to the previous literature will be discussed in the following section.

DISCUSSION AND CONCLUSIONS

How does our presently determined value of 0.76 ± 0.02 b for the ^{111}Cd quadrupole moment relate to the one determined a few years ago by Haas and Correia,[25] 0.765 ± 0.015 b? The values as well as the error bars are very similar, which apparently suggests that there is not much new information in the present study. We argue, however, that this good agreement is fortuitous, and that the error bar proposed by Haas and Correia can only be partially justified. The arguments are as follows: (1) Their 0.765 b quadrupole moment is entirely determined by the DFT prediction of V_{zz} in hcp-Cd only. This makes the value sensitive to imperfections in the exchange-correlation functional that are specific for this crystal, and that could perhaps have different effects in other classes of crystals. The 0.015 b error bar too is determined exclusively by the numerical uncertainty on the V_{zz} prediction for hcp-Cd, which they estimate to be 2% without documenting the procedure. (2) The slope of the (ν_Q, V_{zz})-correlation determined from the low-temperature value of ν_Q for hcp-Cd is found by Haas and Correia to be in excellent agreement with room-temperature data for four other crystals ($CdCl_2$ from ref 37, $CdSiP_2$ from ref 99, $CdSnP_2$ and $CdGeP_2$ from ref 100). This is actually a worrisome observation, given the temperature dependence of ν_Q discussed in the experimental part of the Data Set section.

To remediate these concerns, we considered seven different crystals in our analysis, with experimental data all taken at low temperatures. In principle, it would indeed be sufficient to have just one crystal for which the low-temperature lattice parameters, the low-temperature ν_Q, as well as the calculated V_{zz} are very precisely determined. That would lead in a less complicated way to a lower error bar on the quadrupole moment. Such a procedure has been followed, for instance, to determine the quadrupole moment of ^{14}N to be 0.02044(3) b ("perhaps the most accurate *Q* value known" according to ref 15), obtained either from an excited state of the N ion[101] or from the diatomic NP molecule.[102] This atomic or molecular route to the quadrupole moment, however, requires the applicability of quantum chemistry methods to determine the electric-field gradient (see also the discussion at the end of the section on the Error Budget). In contrast to density functional theory, these methods can in principle approach absolute accuracy for V_{zz}. Density functional theory, on the other hand, is limited by the (unknown) limitations of the chosen exchange-correlation functional. Even when several exchange-correlation functionals are used to assess the possible spread, as was done in this work, and when they are found to be in good agreement with each other, there is no guarantee that the obtained predictions for V_{zz} come anyhow close to the true value. It is, for example, possible that due to a particular form of electron behavior that semilocal exchange-correlation functionals cannot describe, the predicted V_{zz} for a particular material is far from the experimental value. The only way to be reasonably safe against such DFT artifacts due to the functional is to spread the risk over many cases: whereas an erroneous prediction of V_{zz} by some factor x is possible for one solid, it is unlikely that the same factor will apply to seven different solids. This enables outlier detection (see the section on Outlier Assessment), and the remaining, slightly differently erroneous predictions will blend into a larger overall error bar. A possibly remaining systematic deviation, however, will not be detectable.

One way to assess such a possible bias due to the choice of exchange-correlation functional, is to compare our value for this quadrupole moment to a value that does not rely on density-funtional theory. This can be done by repeating the analysis from Herzog et al.[28] that was discussed at the end of the introduction, but starting from the recently determined quadrupole moment of the $11/2^-$ level by Yordanov et al.:[45] −0.747(30) b, by a combination of laser spectroscopy and quantum chemistry. This value should be more accurate and precise than the 1969 value[32] of −0.85(9) b that was used by Herzog et al. Plugging the new value into eq 2 together with the experimental quadrupole coupling constants $\nu_Q(11/2^-) = -139(15)$ MHz (ref 28) and $\nu_Q(5/2^+) = -136.5(1.4)$ MHz (ref 61) (both for hcp-Zn as host material), we obtain for the 245 keV $5/2^+$ level of ^{111}Cd 0.73(8) b (gray circle at the right-hand side of Figure 2). This value does not depend on density functional theory, only on quantum chemistry and experiment. It is entirely consistent (i.e., overlapping uncertainties) with our 0.76(2) b obtained from DFT and experiment, yet tends to be somewhat smaller than the DFT value. This could be an indication that the V_{zz} values as predicted by DFT are indeed a few percent (5%?) too small, consistent with the observations made at the end of the section on the Error Budget.

Finally, we now demonstrate how these two differently determined values for the $5/2^+$ quadrupole moment of ^{111}Cd serve as a litmus test to inspect the difference between DFT and quantum chemistry calculations of V_{zz}, without the need to apply both types of calculations to the same system. For a typical value of $\nu_Q = 135$ MHz, the difference between V_{zz} obtained via our DFT quadrupole moment and V_{zz} obtained by the quantum chemistry quadrupole moment is 0.3×10^{21} V/m^2 or 4%. That is comparable to the numerical uncertainty on V_{zz} when calculated by DFT (see the Analysis section). Because of the largely overlapping error bars on the DFT and the quantum chemistry *Q*, one cannot conclude whether or not the difference in V_{zz} predictions is significant. If the error bar of 0.08 b on the "quantum chemistry Q($5/2^+$)" could be further reduced, one would have a very clean case to examine the otherwise undetectable systematic deviation on V_{zz}-values

DOI: 10.1021/acs.jpcc.6b06127
J. Phys. Chem. C 2016, 120, 23111−23120

determined by DFT. Not directly, which would require DFT and quantum chemistry calculations on exactly the same systems, which is often not possible, but indirectly, through the quadrupole moment. The major contribution to this 0.08 b error bar is due to the 15 MHz uncertainty on the $11/2^-$ quadrupole coupling constant of Cd in hcp-Zn measured by nuclear orientation (ref 28). If this could be reduced to 1 MHz, something that is certainly achievable by modern equipment, the error bar on the quantum chemistry $Q(5/2^+)$ would reduce to 0.03 b. The second most important contribution stems from the error on the quantum chemistry $Q(11/2^-)$ itself. This can be reduced by performing multiconfiguration Dirac–Hartree–Fock calculations for the $^3P_2$ or $^2P_{3/2}$ states of the free Cd atom, going further in the configuration interaction expansion than has been done so far.[45,96] Reducing in this way the error bar on the quantum chemistry $Q(5/2^+)$ to 0.02 b or better would make the comparison between the DFT and quantum chemistry values of V_{zz} sensitive to differences of about 0.2 × 10^{21} V/m^2 or 3%.

In conclusion, we claim that the value with error bar of 0.76(2) b for the nuclear electric quadrupole moment of the $5/2^+$ level of ^{111}Cd is the most accurate and most precise value that can be achieved by semilocal exchange-correlation functionals in density functional theory. This precise determination complements recent efforts[45,96] to determine quadrupole moments of long-lived levels of Cd isotopes (the short-lived $5/2^+$ level is not suitable for laser spectroscopy experiments as in the previous studies). The value we found is slightly lower than the experimental value that is most often quoted, yet consistent with a reanalysis of that experiment based on a recently determined reference quadrupole moment that depends on experiment and independent quantum chemistry calculations. More importantly, our value comes with a well-justified error bar. It is an inherent limitation of the solid-state density functional theory approach to quadrupole moments that this error bar cannot detect systematic deviations that are due to limitations of the exchange-correlation functional. We try to minimize this limitation by using information from seven different crystals, and the agreement of our value with an independent value based on experiment and quantum chemistry indicates that indeed this systematic deviation cannot be large. If anything, the presently proposed quadrupole moment could be a few percent too large. Suggestions for nuclear orientation experiments and quantum chemistry calculations are given that can lead to an even more precise comparison between DFT and quantum chemistry predictions for V_{zz}. Up to date, nuclear model calculations to predict this quadrupole moment directly from nuclear physics theory would be another way to shed new light on this topic.

AUTHOR INFORMATION

Corresponding Author

*E-mail: stefaan.cottenier@ugent.be.

Notes

The authors declare no competing financial interest.

ACKNOWLEDGMENTS

This work was performed under project G.0E01.16N of the Research Foundation - Flanders (FWO), and was supported by the MINCyT-FWO program FW/14/03-VS.020.15N, the MINCyT-DAAD grant DA13/02, UNNOBA, and Consejo Nacional de Investigaciones Científicas y Técnicas (CONICET) under PIP60002. K.L. acknowledges financial support from the Research Board of Ghent University (BOF). S.C. acknowledges financial support from OCAS NV by an OCAS-endowed chair at Ghent University. Calculations were carried out using the Stevin Supercomputer Infrastructure at Ghent University (funded by Ghent University, the Flemish Supercomputer Center (VSC), and the Research Foundation - Flanders (FWO)), the HP-Parallel-Computing Bose Cluster and computational facilities at IFLP and Departamento de Física (UNLP), and the Huge Cluster, University of Aarhus, Denmark. S.C. and S.N.M. acknowledge inspiring discussions with Michel Rots (KU Leuven, Belgium) about TDPAC and quadrupole moments. S.C. thanks the Tata Institute of Fundamental Research (TIFR, Mumbai, India) for enabling a research stay at TIFR that allowed finalizing this work. E.L., M.R. and S.C. dedicate this work to the memory of Axel Svane, a long-time researcher in this field (see e.g., ref 20) who recently passed away.

REFERENCES

(1) Slichter, C. P. *Principles of Magnetic Resonance*; Springer: New York, 1990.
(2) Yoshida, Y., Langouche, G., Eds. *Mössbauer Spectroscopy - Tutorial Book*; Springer: New York, 2013.
(3) Mahnke, H. E. Introduction to PAC/PAD. *Hyperfine Interact.* **1989**, *49*, 77–102.
(4) Schatz, G.; Weidinger, A. *Nuclear Condensed Matter Physics: Nuclear Methods and Applications*; Wiley: New York, 1995.
(5) Krien, K.; Reuschenbach, F.; Soares, J. C.; Herzog, P.; Folle, H. R.; Perscheid, B.; Trzcinski, R.; Freitag, K.; Kaufmann, E. N. The Electric Field Gradients for Hg at Different Lattice Sites in Be. *Hyperfine Interact.* **1979**, *7*, 401–412.
(6) Klas, T.; Voigt, J.; Keppner, W.; Wesche, R.; Schatz, G. Characterization of Copper (100) Surfaces by Isolated Indium Probe Atoms via the Electric Field Gradient. *Phys. Rev. Lett.* **1986**, *57*, 1068–1971.
(7) Denninger, G.; Reiser, D. Determination of Electric-Field Gradients in Semiconductors with High Precision and High Sensitivity. *Phys. Rev. B: Condens. Matter Mater. Phys.* **1997**, *55*, 5073–5078.
(8) Potzger, K.; Weber, A.; Bertschat, H. H.; Zeitz, W. D.; Dietrich, M. Coordination-Number Dependence of Magnetic Hyperfine Fields at ^{111}Cd on Ni Surfaces. *Phys. Rev. Lett.* **2002**, *88*, 247201.
(9) Errico, L. A.; Fabricius, G.; Rentería, M.; de la Presa, P.; Forker, M. Anisotropic Relaxations Introduced by Cd Impurities in Rutile TiO_2: First-Principles Calculations and Experimental Support. *Phys. Rev. Lett.* **2002**, *89*, 055503.
(10) Richard, D.; Muñoz, E. L.; Rentería, M.; Errico, L. A.; Svane, A.; Christensen, N. E. Ab Initio LSDA and LSDA+U Study of Pure and Cd-Doped Cubic Lanthanide Sesquioxides. *Phys. Rev. B: Condens. Matter Mater. Phys.* **2013**, *88*, 165206.
(11) Lupascu, D.; Uhrmacher, M.; Lieb, K. P. Electric Field Gradients of ^{111}Cd in Monoclinic (B-phase) Rare Earth Sesquioxides. *J. Phys.: Condens. Matter* **1994**, *6*, 10445–10456.
(12) Rentería, M.; Errico, L. A.; Bibiloni, A. G.; Freitag, K.; Requejo, F. G. PAC Identification of Electric-Nuclear-Quadrupole Interactions in Sm-Sesquioxides. *Z. Naturforsch., A: Phys. Sci.* **2000**, *55*, 155–159.
(13) Tsvyashchenko, A. V.; Fomicheva, L. N.; Velichkov, A.; Salamatin, A.; Kochetov, O. I.; Ryasny, G.; Nikolaev, A.; Budzynski, M.; Spasskiy, A. V. ^{111}Cd-Time Differential Perturbed Angular Correlation Study of Pressure Effect on the Hyperfine Quadrupole Interaction in the UGe_2 Cubic Phase. *J. Alloys Compd.* **2012**, *541*, 234–237.
(14) Stone, N. J. Table of Nuclear Magnetic Dipole and Electric Quadrupole Moments. *At. Data Nucl. Data Tables* **2005**, *90*, 75–176.
(15) Pyykkö, P. Year-2008 Nuclear Quadrupole Moments. *Mol. Phys.* **2008**, *106*, 1965–1974.

DOI: 10.1021/acs.jpcc.6b06127
J. Phys. Chem. C 2016, 120, 23111–23120

(16) Stone, N. J. Table of Nuclear Magnetic Dipole and Electric Quadrupole Moments. International Nuclear Data Committee, 2014; https://www-nds.iaea.org/publications/indc/indc-nds-0658.pdf, last accessed September 2016.
(17) Stone, N. J. Table of Nuclear Electric Quadrupole Moments. International Nuclear Data Committee, 2014; https://www-nds.iaea.org/publications/indc/indc-nds-0650.pdf, last accessed September 2016.
(18) Dufek, P.; Blaha, P.; Schwarz, K. Determination of the Nuclear Quadrupole Moment of ^{57}Fe. *Phys. Rev. Lett.* **1995**, *75*, 3545−3548.
(19) Blaha, P.; Dufek, P.; Schwarz, K.; Haas, H. Calculation of Electric Hyperfine Interaction Parameters in Solids. *Hyperfine Interact.* **1996**, *97*, 1−10.
(20) Svane, A.; Christensen, N. E.; Rodriguez, C.; Methfessel, M. Calculations of Hyperfine Parameters in Tin Compounds. *Phys. Rev. B: Condens. Matter Mater. Phys.* **1997**, *55*, 12572−12577.
(21) Balabanski, D. L.; Vyvey, K.; Neyens, G.; Coulier, N.; Coussement, R.; Georgiev, G.; Lèpine-Szily, A.; Ternier, S.; Teughels, S.; Mineva, M.; et al. Static Quadrupole Moment of the Five-Quasiparticle K = 35/2 Isomer in ^{179}W Studied with the Level-Mixing Spectroscopy Method. *Phys. Rev. Lett.* **2001**, *86*, 604−607.
(22) Errico, L.; Rentería, M. Ab Initio Determination of the Nuclear Quadrupole Moments of ^{114}In, ^{115}In, and ^{117}In. *Phys. Rev. B: Condens. Matter Mater. Phys.* **2006**, *73*, 115125.
(23) Ryu, S. B.; Das, S. K.; Butz, T.; Schmitz, W.; Spiel, C.; Blaha, P.; Schwarz, K. Nuclear Quadrupole Interaction at ^{44}Sc in the Anatase and Rutile Modifications of TiO_2: Time-Differential Perturbed-Angular-Correlation Measurements and Ab Initio Calculations. *Phys. Rev. B: Condens. Matter Mater. Phys.* **2008**, *77*, 094124.
(24) Errico, L.; Darriba, G.; Rentería, M.; Tang, Z.; Emmerich, H.; Cottenier, S. Nuclear Quadrupole Moment of the ^{99}Tc Ground State. *Phys. Rev. B: Condens. Matter Mater. Phys.* **2008**, *77*, 195118.
(25) Haas, H.; Correia, J. G. The Quadrupole Moments of Zn and Cd Isotopes − an Update. *Hyperfine Interact.* **2010**, *198*, 133−137.
(26) Chevrier, R.; Daugas, J. M.; Gaudefroy, L.; Ichikawa, Y.; Ueno, H.; Hass, M.; Haas, H.; Cottenier, S.; Aoi, N.; Asahi, K.; et al. Is the 7/2_1^- Isomer State of ^{43}S Spherical? *Phys. Rev. Lett.* **2012**, *108*, 162501.
(27) van der Werf, D.; van Leuken, H.; de Groot, R. A. Electric-Field-Gradient Calculations on Cadmium in Cadmium-Helium Vacancy Clusters in Tungsten. *Phys. Rev. B: Condens. Matter Mater. Phys.* **1995**, *52*, 3909−3916.
(28) Herzog, P.; Freitag, K.; Reuschenbach, M.; Walitzki, H. Nuclear Orientation of ^{111m}Cd in Zn and Be and the Quadrupole Moment of the 245 keV State. *Z. Phys. A: At. Nucl.* **1980**, *294*, 13−15.
(29) Hemmingsen, L.; Ryde, U. Ab Initio Calculations of Electric Field Gradients in Cadmium Complexes. *J. Phys. Chem.* **1996**, *100*, 4803−4809.
(30) Antony, J.; Hansen, B.; Hemmingsen, L.; Bauer, R. Density Functional Calculation of the Electric Field Gradient in Cadmium Complexes: Comparison with Hartree-Fock, Second-Order Møller-Plesset, and Experimental Results. *J. Phys. Chem. A* **2000**, *104*, 6047−6055.
(31) Sprouse, G. D.; Häusser, O.; Andrews, H. R.; Faestermann, T.; Beene, J. R.; Alexander, T. K. Static Quadrupole Moments in Cd Isotopes. *Hyperfine Interact.* **1978**, *4*, 229−233.
(32) Laulainen, N. S.; McDermott, M. N. Spin and Nuclear Moments of 55-min Cd^{105} and 49-min Cd^{111m}. *Phys. Rev.* **1969**, *177*, 1615−1623.
(33) Behrend, H.-J.; Budnick, D. Die Bestimmung des Kern-Quadrupolmomentes des 247 keV-Niveaus des Cadmium-111 durch Messung der zirkularen Polarisation der γ-Strahlung. *Eur. Phys. J. A* **1962**, *168*, 155−168.
(34) Kisslinger, L. S.; Sorensens, R. A. Spherical Nuclei with Simple Residual Forces. *Rev. Mod. Phys.* **1963**, *35*, 853−915.
(35) Bodenstedt, E.; Ortabasi, U.; Ellis, W. H. Perturbed-Angular-Correlation Studies of the Quadrupole Interactions of ^{111}Cd in Different Metallic Environments and the Electric Quadrupole Moment of the 247 keV State. *Phys. Rev. B* **1972**, *6*, 2909−2922.
(36) Raghavan, R. S.; Raghavan, P.; Friedt, J. M. Nuclear Quadrupole Interactions of the Excited States of ^{117}In and ^{111}Cd in Cd Compounds. *Phys. Rev. Lett.* **1973**, *30*, 10−13.
(37) Haas, H.; Shirley, D. A. Nuclear Quadrupole Interaction Studies by Perturbed Angular Correlations. *J. Chem. Phys.* **1973**, *58*, 3339−3355.
(38) Sharma, A. K.; Sharma, R. R. Theory of Ligand Distortions−Application to the Study of Nuclear Quadrupole Interactions of the Excited States of ^{111}Cd and ^{117}In in $CdCl_2$. *Phys. Rev. B* **1974**, *10*, 3792−3801.
(39) Rosenblum, S. S.; Steyert, W. A. The Electric Field Gradient in Cadmium Metal and the Decay of ^{115}Cd-m. *Phys. Lett. A* **1975**, *53*, 34−36.
(40) Echt, O.; Haas, H.; Ivanov, E.; Recknagel, E.; Schlodder, E.; Spellmeyer, B. Quadrupole Interaction of ^{107}Cd 2/11$^-$ in Cadmium Metal. *Hyperfine Interact.* **1976**, *2*, 230−231.
(41) Pattnaik, P. C.; Thompson, M. D.; Das, T. P. Ab Initio Theory of Nuclear-Quadrupole Antishielding Effects in Metallic Systems − Application to Zinc and Cadmium. *Phys. Rev. B* **1977**, *16*, 5390−5393.
(42) Thompson, M. D.; Das, T. P.; Ciobanu, G. Theory of Nuclear Quadrupole Interaction in Cadmium Using a First-Principles Pseudopotential. *Phys. Rev. B: Condens. Matter Mater. Phys.* **1979**, *19*, 4328−4330.
(43) Ernst, H.; Hagn, E.; Zech, E. Nuclear Orientation of ^{109}Cd and ^{115m}Cd in Cd. *Phys. Lett. A* **1983**, *93*, 357−359.
(44) Blaha, P.; Schwarz, K.; Dederichs, P. H. First-Principles Calculation of the Electric-Field Gradient in hcp Metals. *Phys. Rev. B: Condens. Matter Mater. Phys.* **1988**, *37*, 2792−2796.
(45) Yordanov, D. T.; Balabanski, D. L.; Bieroń, J.; Bissell, M. L.; Blaum, K.; Budinčević, I.; Fritzsche, S.; Frömmgen, N.; Georgiev, G.; Geppert, C.; et al. Spins, Electromagnetic Moments, and Isomers of $^{107-129}$Cd. *Phys. Rev. Lett.* **2013**, *110*, 192501.
(46) Mortensen, J. J.; Kaasbjerg, K.; Frederiksen, S. L.; Nørskov, J. K.; Sethna, J. P.; Jacobsen, K. W. Bayesian Error Estimation in Density-Functional Theory. *Phys. Rev. Lett.* **2005**, *95*, 216401.
(47) Lejaeghere, K.; Van Speybroeck, V.; Van Oost, G.; Cottenier, S. *Crit. Rev. Solid State Mater. Sci.* **2014**, *39*, 1−24.
(48) Pernot, P.; Civalleri, B.; Presti, D.; Savin, A. Prediction Uncertainty of Density Functional Approximations for Properties of Crystals with Cubic Symmetry. *J. Phys. Chem. A* **2015**, *119*, 5288−5304.
(49) Gaiduk, A. P.; Gygi, F.; Galli, G. Density and Compressibility of Liquid Water and Ice from First-Principles Simulations with Hybrid Functionals. *J. Phys. Chem. Lett.* **2015**, *6*, 2902−2908.
(50) Lejaeghere, K.; Bihlmayer, G.; Björkman, T.; Blaha, P.; Blügel, S.; Blum, V.; Caliste, D.; Castelli, I. E.; Clark, S. J.; Dal Corso, A.; et al. Reproducibility in Density Functional Theory Calculations of Solids. *Science* **2016**, *351*, aad3000.
(51) De Waele, S.; Lejaeghere, K.; Sluydts, M.; Cottenier, S. *Phys. Rev. B* **2016**, submitted.
(52) Barrett, C. S.; Spooner, F. J. Lattice Constants of Gallium at 297 K. *Nature* **1965**, *207*, 1382−1382.
(53) Keppner, W.; Körner, W.; Heubes, P.; Schatz, G. Temperature Dependence of the Electric Field Gradient at ^{111}Cd in Ga- and Bi-Metal. *Hyperfine Interact.* **1981**, *9*, 293−296.
(54) Barrett, C. S. The Structure of Mercury at Low Temperatures. *Acta Crystallogr.* **1957**, *10*, 58−60.
(55) Hewitt, R. R.; Taylor, T. T. Nuclear Quadrupole Resonance and the Electric Field Gradient in Metallic Indium. *Phys. Rev.* **1962**, *125*, 524−532.
(56) Christiansen, J.; Heubes, P.; Keitel, R.; Loeffler, W.; Sandner, W.; Witthuhn, W. Temperature Dependence of the Electric Field Gradient in Noncubic Metals. *Z. Phys. B: Condens. Matter Quanta* **1976**, *24*, 177−187.
(57) Raynne, J. A.; Chandrasekhar, B. S. Elastic Constants of β Tin from 4.2 K to 300 K. *Phys. Rev.* **1960**, *120*, 1658−1663.
(58) Barrett, C. S.; Cucka, P.; Haefner, K. The crystal structure of antimony at 4.2, 78 and 298 K. *Acta Crystallogr.* **1963**, *16*, 451−453.

DOI: 10.1021/acs.jpcc.6b06127
J. Phys. Chem. C 2016, 120, 23111−23120

(59) Lis, S. A.; Naumann, R. A. Temperature Dependence Study of the Quadrupole Interaction of ^{111}Cd in Antimony. *Hyperfine Interact.* **1977**, *3*, 283−286.
(60) Nuss, J.; Wedig, U.; Kirfel, A.; Jansen, M. The Structural Anomaly of Zinc: Evolution of Lattice Constants and Parameters of Thermal Motion in the Temperature Range of 40 to 500 K. *Z. Anorg. Allg. Chem.* **2010**, *636*, 309−313.
(61) Raghavan, P.; Raghavan, R. S.; Kaufmann, E. N.; Krien, K.; Naumann, R. A. Nuclear Quadrupole Interaction of ^{111}Cd in Zinc (by PAC). *J. Phys. F: Met. Phys.* **1974**, *4*, L80−83.
(62) Jena, P. Temperature Dependence of Electric Field Gradients in Noncubic Metals. *Phys. Rev. Lett.* **1976**, *36*, 418−421.
(63) Nishiyama, K.; Dimmling, F.; Kornrumpf, T.; Riegel, D. Theory of the Temperature Dependence of the Electric Field Gradient in Noncubic Metals. *Phys. Rev. Lett.* **1976**, *37*, 357−360.
(64) Torgeson, D. R.; Borsa, F. Temperature Dependence of the Electric Field Gradient in a Quasi-Two-Dimensional Metal: $NbSe_2$. *Phys. Rev. Lett.* **1976**, *37*, 956−959.
(65) Thompson, M. D.; Pattnaik, P. C.; Das, T. P. Temperature-Dependent Field Gradients in Zn and Cd: First-Principles Analysis of Electronic and Lattice Contributions. *Phys. Rev. B: Condens. Matter Mater. Phys.* **1978**, *18*, 5402−5409.
(66) Lodge, K. W. On The Temperature Dependence and Magnitude of the Electric Field Gradient in Noncubic Metals. *J. Phys. F: Met. Phys.* **1979**, *9*, 2035−2048.
(67) Verma, H. C.; Rao, G. N. Systematic Study of the Temperature Dependence of Electric Field Gradients at Probe Nuclei in Non-Cubic Metals. *Hyperfine Interact.* **1983**, *15*, 207−210.
(68) Torumba, D.; Parlinski, K.; Rots, M.; Cottenier, S. Temperature Dependence of the Electric-Field Gradient in hcp-Cd from First Principles. *Phys. Rev. B: Condens. Matter Mater. Phys.* **2006**, *74*, 144304.
(69) Blaha, P.; Schwarz, K.; Madsen, G. K. H.; Kvasnicka, D.; Luitz, J. *WIEN2k, An Augmented Plane Wave + Local Orbitals Program for Calculating Crystal Properties*; Karlheinz Schwarz, Techn. Universität Wien: Austria, 2001.
(70) Blaha, P.; Schwarz, K.; Herzig, P. First-Principles Calculation of the Electric Field Gradient of Li_3N. *Phys. Rev. Lett.* **1985**, *54*, 1192−1195.
(71) Jalali Asadabadi, S.; Cottenier, S.; Akbarzadeh, H.; Saki, R.; Rots, M. Valency of rare earths in RIn_3 and RSn_3: Ab initio analysis of electric-field gradients. *Phys. Rev. B: Condens. Matter Mater. Phys.* **2002**, *66*, 195103.
(72) Hansen, M. R.; Madsen, G. K. H.; Jakobsen, H. J.; Skibsted, J. Refinement of Borate Structures from ^{11}B MAS NMR Spectroscopy and Density Functional Theory Calculations of ^{11}B Electric Field Gradients. *J. Phys. Chem. A* **2005**, *109*, 1989−1997.
(73) Body, M.; Legein, C.; Buzare, J. Y.; Silly, G.; Blaha, P.; Martineau, C.; Calvayrac, F. Advances in Structural Analysis of Fluoroaluminates Using DFT Calculations of ^{27}Al Electric Field Gradients. *J. Phys. Chem. A* **2007**, *111*, 11873−11884.
(74) Torumba, D.; Novák, P.; Cottenier, S. Hybrid Exchange-Correlation Functionals Applied to Hyperfine Interactions at Lanthanide and Actinide Impurities in Fe. *Phys. Rev. B: Condens. Matter Mater. Phys.* **2008**, *77*, 155101.
(75) Hanna, J. V.; Pike, K. J.; Charpentier, T.; Kemp, T. F.; Smith, M. E.; Lucier, B. E. G.; Schurko, R. W.; Cahill, L. S. A ^{93}Nb Solid-State NMR and Density Functional Theory Study of Four- and Six-Coordinate Niobate Systems. *Chem. - Eur. J.* **2010**, *16*, 3222−3239.
(76) Schwarz, K.; Blaha, P.; Trickey, S. B. Electronic Structure of Solids with WIEN2k. *Mol. Phys.* **2010**, *108*, 3147−3166.
(77) Sjöstedt, E.; Nordström, L.; Singh, D. J. An Alternative Way of Linearizing the Augmented Plane-Wave Method. *Solid State Commun.* **2000**, *114*, 15−20.
(78) Madsen, G. K. H.; Blaha, P.; Schwarz, K.; Sjöstedt, E.; Nordström, L. Efficient linearization of the augmented plane-wave method. *Phys. Rev. B: Condens. Matter Mater. Phys.* **2001**, *64*, 195134.
(79) Cottenier, S. *Density Functional Theory and the Family of (L)APW-methods: a step-by-step introduction*; Instituut voor Kern- en Stralingsfysica: KU Leuven, Belgium, 2002; (to be found at http://www.wien2k.at/reg_user/textbooks, last accessed September 2016).
(80) Lejaeghere, K.; Jaeken, J.; Van Speybroeck, V.; Cottenier, S. Ab Initio Based Thermal Property Predictions at a Low Cost: An Error Analysis. *Phys. Rev. B: Condens. Matter Mater. Phys.* **2014**, *89*, 014304.
(81) Cook, R. D.; Weisberg, S. *Residuals and Influence in Regression (Monographs on Statistics and Applied Probability, 18)*; Chapman and Hall: New York-London, 1982.
(82) Borcherds, P. H.; Sheth, C. V. Least Squares Fitting of a Straight line to a Set of Data Points. *Eur. J. Phys.* **1995**, *16*, 204−210.
(83) Sheth, C. V.; Ngwengwe, A.; Borcherds, P. H. Least Squares Fitting of a Straight Line to a Set of Data Points: II. Parameter Variances. *Eur. J. Phys.* **1996**, *17*, 322−326.
(84) Thyssen, J.; Schwerdtfeger, P.; Bender, M.; Nazarewicz, W.; Semmes, P. B. Quadrupole and Hexadecapole Couplings for ^{127}I in $Li^{127}I$. *Phys. Rev. A: At., Mol., Opt. Phys.* **2001**, *63*, 022505.
(85) Koch, K.; Koepernik, K.; Van Neck, D.; Rosner, H.; Cottenier, S. Electron Penetration into the Nucleus and its Effect on the Quadrupole Interaction. *Phys. Rev. A: At., Mol., Opt. Phys.* **2010**, *81*, 032507.
(86) Rose, K.; Cottenier, S. Classical Toy Models for the Monopole Shift and the Quadrupole Shift. *Phys. Chem. Chem. Phys.* **2012**, *14*, 11308−11317.
(87) Filatov, M.; Zou, W. L.; Cremer, D. Communication: On the Isotope Anomaly of Nuclear Quadrupole Coupling in Molecules. *J. Chem. Phys.* **2012**, *137*, 131102.
(88) Perdew, J. P.; Wang, Y. Accurate and Simple Analytic Representation of the Electron-Gas Correlation Energy. *Phys. Rev. B: Condens. Matter Mater. Phys.* **1992**, *45*, 13244−13249.
(89) Wu, Z.; Cohen, R. E. More Accurate Generalized Gradient Approximation for Solids. *Phys. Rev. B: Condens. Matter Mater. Phys.* **2006**, *73*, 235116.
(90) Perdew, J. P.; Ruzsinszky, A.; Csonka, G. I.; Vydrov, O. A.; Scuseria, G. E.; Constantin, L. A.; Zhou, X.; Burke, K. Restoring the Density-Gradient Expansion for Exchange in Solids and Surfaces. *Phys. Rev. Lett.* **2008**, *100*, 136406.
(91) Pyykkö, P.; Seth, M. Relativistic Effects in Nuclear Quadrupole Coupling. *Theor. Chem. Acc.* **1997**, *96*, 92−104.
(92) Pernpointner, M.; Schwerdtfeger, P. Spin-Orbit Effects in Electric Field Gradients of Alkali Metal Atoms. *J. Phys. B: At., Mol. Opt. Phys.* **2001**, *34*, 659−670.
(93) Seewald, G.; Hagn, E.; Zech, E.; Kleyna, R.; Voss, M.; Burchard, A. Spin-Orbit Induced Noncubic Charge Distribution in Cubic Ferromagnets. I. Electric Field Gradient Measurements on 5d Impurities in Fe and Ni. *Phys. Rev. B: Condens. Matter Mater. Phys.* **2002**, *66*, 174401.
(94) Arcisauskaite, V.; Knecht, S.; Sauer, S. P. A.; Hemmingsen, L. Electric Field Gradients in Hg Compounds: Molecular Orbital (MO) Analysis and Comparison of 4-Component and 2-Component (ZORA) Methods. *Phys. Chem. Chem. Phys.* **2012**, *14*, 16070−16079.
(95) Autschbach, J.; Peng, D.; Reiher, M. Two-Component Relativistic Calculations of Electric-Field Gradients Using Exact Decoupling Methods: Spin-orbit and Picture-Change Effects. *J. Chem. Theory Comput.* **2012**, *8*, 4239−4248.
(96) Frömmgen, N.; Balabanski, D. L.; Bissell, M. L.; Bieroń, J.; Blaum, K.; Cheal, B.; Flanagan, K.; Fritzsche, S.; Geppert, C.; Hammen, M.; et al. Collinear Laser Spectroscopy of Atomic Cadmium Extraction of Nuclear Magnetic Dipole and Electric Quadrupole Moments. *Eur. Phys. J. D* **2015**, *69*, 164.
(97) Soldner, T.; Tröger, W.; Butz, T.; Blaha, P.; Schwarz, K. Calculation of Electric Field Gradients in Isolated Molecules Using the FPLAPW-Code WIEN95. *Z. Naturforsch., A: Phys. Sci.* **1998**, *53*, 411−418.
(98) Arcisauskaite, V.; Knecht, S.; Sauer, S. P. A.; Hemmingsen, L. Fully Relativistic Coupled Cluster and DFT Study of Electric Field Gradients at Hg in ^{199}Hg compounds. *Phys. Chem. Chem. Phys.* **2012**, *14*, 2651−2657.
(99) Unterricker, S.; Hausbrand, J. PAC Examination of Radiation Damaged $CdSiP_2$. *Phys. Status Solidi (a)* **1978**, *46*, 125−130.

DOI: 10.1021/acs.jpcc.6b06127
J. Phys. Chem. C 2016, 120, 23111−23120

(100) Unterricker, S.; Schneider, F. The EFG Lattice Structure Dependence of Cd on A-sites in A(II)B(IV)C(V)$_2$-semiconductors. *Hyperfine Interact.* **1983**, *15/16*, 827−830.
(101) Tokman, M.; Sundholm, D.; Pyykkö, P.; Olsen, J. The Nuclear Quadrupole Moment of ^{14}N Obtained from Finite-Element MCHF Calculations on N^{2+} (2p; $^2P_{3/2}$) and $N^+(2p^2; {}^3P_2$ and $2p^2; {}^1D_2)$. *Chem. Phys. Lett.* **1997**, *265*, 60−64.
(102) Kellö, V.; Sadlej, A. J. The Nuclear Quadrupole Moment of ^{14}N from Accurate Electric Field Gradient Calculations and Microwave Spectra of NP Molecule. *Collect. Czech. Chem. Commun.* **2007**, *72*, 64−82.

DOI: 10.1021/acs.jpcc.6b06127
J. Phys. Chem. C 2016, 120, 23111−23120